JOURNAL OF Applied Polymer SCIENCE

Special Issue: Bio-based Packaging

Guest Editors: José M. Lagarón, Amparo López-Rubio, and María José Fabra
Institute of Agrochemistry and Food Technology of the Spanish Council for Scientific Research

EDITORIAL

Bio-based Packaging
J. M. Lagarón, A. López-Rubio and M. J. Fabra, *J. Appl. Polym. Sci.* 2015, DOI: 10.1002/app.42971

REVIEWS

Active edible films: Current state and future trends
C. Mellinas, A. Valdés, M. Ramos, N. Burgos, M. D. C. Garrigós and A. Jiménz, *J. Appl. Polym. Sci.* 2015, DOI: 10.1002/app.42631

Vegetal fiber-based biocomposites: Which stakes for food packaging applications?
M.-A. Berthet, H. Angellier-Coussy, V. Guillard and N. Gontard, *J. Appl. Polym. Sci.* 2015, DOI: 10.1002/app.42528

Enzymatic-assisted extraction and modification of lignocellulosic plant polysaccharides for packaging applications
A. Martínez-Abad, A. C. Ruthes and F. Vilaplana, *J. Appl. Polym. Sci.* 2015, DOI: 10.1002/app.42523

RESEARCH ARTICLES

Combining polyhydroxyalkanoates with nanokeratin to develop novel biopackaging structures
M. J. Fabra, P. Pardo, M. Martínez-Sanz, A. Lopez-Rubio and J. M. Lagarón, *J. Appl. Polym. Sci.* 2015, DOI: 10.1002/app.42695

Production of bacterial nanobiocomposites of polyhydroxyalkanoates derived from waste and bacterial nanocellulose by the electrospinning enabling melt compounding method
M. Martínez-Sanz, A. Lopez-Rubio, M. Villano, C. S. S. Oliveira, M. Majone, M. Reis and J. M. Lagarón, *J. Appl. Polym. Sci.* 2015, DOI: 10.1002/app.42486

Bio-based multilayer barrier films by extrusion, dispersion coating and atomic layer deposition
J. Vartiainen, Y. Shen, T. Kaljunen, T. Malm, M. Vähä-Nissi, M. Putkonen and A. Harlin, *J. Appl. Polym. Sci. 2*015, DOI: 10.1002/app.42260

Film blowing of PHBV blends and PHBV-based multilayers for the production of biodegradable packages
M. Cunha, B. Fernandes, J. A. Covas, A. A. Vicente and L. Hilliou, *J. Appl. Polym. Sci.* 2015, DOI: 10.1002/app.42165

On the use of tris(nonylphenyl) phosphite as a chain extender in melt-blended poly(hydroxybutyrate-*co*-hydroxyvalerate)/clay nanocomposites: Morphology, thermal stability, and mechanical properties
J. González-Ausejo, E. Sánchez-Safont, J. Gámez-Pérez and L. Cabedo, *J. Appl. Polym. Sci.* 2015, DOI: 10.1002/app.42390

Characterization of polyhydroxyalkanoate blends incorporating unpurified biosustainably produced poly(3-hydroxybutyrate-*co*-3-hydroxyvalerate)
A. Martínez-Abad, L. Cabedo, C. S. S. Oliveira, L. Hilliou, M. Reis and J. M. Lagarón, *J. Appl. Polym. Sci.* 2015, DOI: 10.1002/app.42633

Modification of poly(3-hydroxybutyrate-*co*-3-hydroxyvalerate) properties by reactive blending with a monoterpene derivative
L. Pilon and C. Kelly, *J. Appl. Polym. Sci.* 2015, DOI: 10.1002/app.42588

Poly(3-hydroxybutyrate-*co*-3-hydroxyvalerate) films for food packaging: Physical–chemical and structural stability under food contact conditions
V. Chea, H. Angellier-Coussy, S. Peyron, D. Kemmer and N. Gontard, *J. Appl. Polym. Sci.* 2015, DOI: 10.1002/app.41850

JOURNAL OF Applied Polymer SCIENCE

Special Issue: Bio-based Packaging

Guest Editors: José M. Lagarón, Amparo López-Rubio, and María José Fabra
Institute of Agrochemistry and Food Technology of the Spanish Council for Scientific Research

Impact of fermentation residues on the thermal, structural, and rheological properties of polyhydroxy(butyrate-*co*-valerate) produced from cheese whey and olive oil mill wastewater
L. Hilliou, D. Machado, C. S. S. Oliveira, A. R. Gouveia, M. A. M. Reis, S. Campanari, M. Villano and M. Majone, *J. Appl. Polym. Sci.* 2015, DOI: 10.1002/app.42818

Synergistic effect of lactic acid oligomers and laminar graphene sheets on the barrier properties of polylactide nanocomposites obtained by the in situ polymerization pre-incorporation method
J. Ambrosio-Martín, A. López-Rubio, M. J. Fabra, M. A. López-Manchado, A. Sorrentino, G. Gorrasi and J. M. Lagarón, *J. Appl. Polym. Sci.* 2015, DOI: 10.1002/app.42661

Antibacterial poly(lactic acid) (PLA) films grafted with electrospun PLA/allyl isothiocyanate fibers for food packaging
H. H. Kara, F. Xiao, M. Sarker, T. Z. Jin, A. M. M. Sousa, C.-K. Liu, P. M. Tomasula and L. Liu, *J. Appl. Polym. Sci.* 2015, DOI: 10.1002/app.42475

Poly(L-lactide)/ZnO nanocomposites as efficient UV-shielding coatings for packaging applications
E. Lizundia, L. Ruiz-Rubio, J. L. Vilas and L. M. León, *J. Appl. Polym. Sci.* 2015, DOI: 10.1002/app.42426

Effect of electron beam irradiation on the properties of polylactic acid/montmorillonite nanocomposites for food packaging applications
M. Salvatore, A. Marra, D. Duraccio, S. Shayanfar, S. D. Pillai, S. Cimmino and C. Silvestre, *J. Appl. Polym. Sci.* 2015, DOI: 10.1002/app.42219

Preparation and characterization of linear and star-shaped poly L-lactide blends
M. B. Khajeheian and A. Rosling, *J. Appl. Polym. Sci.* 2015, DOI: 10.1002/app.42231

Mechanical properties of biodegradable polylactide/poly(ether-block-amide)/thermoplastic starch blends: Effect of the crosslinking of starch
L. Zhou, G. Zhao and W. Jiang, *J. Appl. Polym. Sci.* 2015, DOI: 10.1002/app.42297

Interaction and quantification of thymol in active PLA-based materials containing natural fibers
I. S. M. A. Tawakkal, M. J. Cran and S. W. Bigger, *J. Appl. Polym. Sci.* 2015, DOI: 10.1002/app.42160

Graphene-modified poly(lactic acid) for packaging: Material formulation, processing, and performance
M. Barletta, M. Puopolo, V. Tagliaferri and S. Vesco, *J. Appl. Polym. Sci.* 2015, DOI: 10.1002/app.42252

Edible films based on chia flour: Development and characterization
M. Dick, C. H. Pagno, T. M. H. Costa, A. Gomaa, M. Subirade, A. De O. Rios and S. H. Flóres, *J. Appl. Polym. Sci.* 2015, DOI: 10.1002/app.42455

Influence of citric acid on the properties and stability of starch-polycaprolactone based films
R. Ortega-Toro, S. Collazo-Bigliardi, P. Talens and A. Chiralt, *J. Appl. Polym. Sci.* 2015, DOI: 10.1002/app.42220

Bionanocomposites based on polysaccharides and fibrous clays for packaging applications
A. C. S. Alcântara, M. Darder, P. Aranda, A. Ayral and E. Ruiz-Hitzky, *J. Appl. Polym. Sci.* 2015, DOI: 10.1002/app.42362

Hybrid carrageenan-based formulations for edible film preparation: Benchmarking with kappa carrageenan
F. D. S. Larotonda, M. D. Torres, M. P. Gonçalves, A. M. Sereno and L. Hilliou, *J. Appl. Polym. Sci.* 2015, DOI: 10.1002/app.42263

JOURNAL OF Applied Polymer SCIENCE

Special Issue: Bio-based Packaging

Guest Editors: José M. Lagarón, Amparo López-Rubio, and María José Fabra
Institute of Agrochemistry and Food Technology of the Spanish Council for Scientific Research

Structural and mechanical properties of clay nanocomposite foams based on cellulose for the food packaging industry
S. Ahmadzadeh, J. Keramat, A. Nasirpour, N. Hamdami, T. Behzad, L. Aranda, M. Vilasi and S. Desobry, *J. Appl. Polym. Sci.* 2015, DOI: 10.1002/app.42079

Mechanically strong nanocomposite films based on highly filled carboxymethyl cellulose with graphene oxide
M. El Achaby, N. El Miri, A. Snik, M. Zahouily, K. Abdelouahdi, A. Fihri, A. Barakat and A. Solhy, *J. Appl. Polym. Sci.* 2015, DOI: 10.1002/app.42356

Production and characterization of microfibrillated cellulose-reinforced thermoplastic starch composites
L. Lendvai, J. Karger-Kocsis, Á. Kmetty and S. X. Drakopoulos, *J. Appl. Polym. Sci.* 2015, DOI: 10.1002/app.42397

Development of bioplastics based on agricultural side-stream products: Film extrusion of *Crambe abyssinica*/wheat gluten blends for packaging purposes
H. Rasel, T. Johansson, M. Gällstedt, W. Newson, E. Johansson and M. Hedenqvist, *J. Appl. Polym. Sci.* 2015, DOI: 10.1002/app.42442

Influence of plasticizers on the mechanical and barrier properties of cast biopolymer films
V. Jost and C. Stramm, *J. Appl. Polym. Sci.* 2015, DOI: 10.1002/app.42513

The effect of oxidized ferulic acid on physicochemical properties of bitter vetch (*Vicia ervilia*) protein-based films
A. Arabestani, M. Kadivar, M. Shahedi, S. A. H. Goli and R. Porta, *J. Appl. Polym. Sci.* 2015, DOI: 10.1002/app.42894

Effect of hydrochloric acid on the properties of biodegradable packaging materials of carboxymethylcellulose/poly(vinyl alcohol) blends
M. D. H. Rashid, M. D. S. Rahaman, S. E. Kabir and M. A. Khan, *J. Appl. Polym. Sci.* 2015, DOI: 10.1002/app.42870

Journal of Applied Polymer Science

Preparation and characterization of linear and star-shaped poly L-lactide blends

Mohammad B. Khajeheian, Ari Rosling
FUNMAT Centre of Excellence, Laboratory of Polymer Technology, Åbo Akademi University, FI-20500 Turku/Åbo, Finland
Correspondence to: A. Rosling (E-mail: arosling@abo.fi)

ABSTRACT: A series of star-shaped poly(L-lactide) (sPLLA) with different branch length was synthesized by ring-opening polymerization of L-lactide using pentaerythritol as initiator and stannous-octoate as catalyst. The structures and properties of the sPLLAs were characterized by ^{1}H-NMR, rheology, differential scanning calorimetry, and size-exclusion chromatography. The star-shaped polymers were blended with a linear PLLA resin (3051D; NatureWorks) and studied for their melt flow and thermal properties. Blends containing 10 wt % of sPLLA displayed equivalent zero shear viscosities to PLLA 3051D, however displaying stronger shear thinning and increased melt elasticity. The blends exhibited also similar thermal and crystallization properties as the PLLA 3051D. A higher ratio of low molecular weight sPLLA (30 wt %; Mw_{total}: 2500 and 15,000 g mol^{-1}) lowered the zero viscosity and increased shear thinning of PLLA 3051D. Crystallization of PLLA 3051D appears to increase at 30 wt % blends with the higher molecular weight sPLLA, while the star-shaped structure acts as a nucleating agent. © 2015 Wiley Periodicals, Inc. J. Appl. Polym. Sci. **2016**, *133*, 42231.

KEYWORDS: biopolymers and renewable polymers; blends; extrusion; rheology; viscosity and viscoelasticity

Received 14 November 2014; accepted 10 March 2015
DOI: 10.1002/app.42231

INTRODUCTION

Over the last decade, rising crude oil price and growing environmental awareness have enhanced motivation toward developing biodegradable polymers from renewable resources.[1–3] Biodegradable polymers have been introduced to various fields as alternatives to traditional polymeric materials. Among all, poly(L-lactide) (PLLA) is one of the most important biodegradable polymers.[4,5] Polylactide has attracted attention as a candidate of non-petroleum-based biodegradable polymeric materials because PLLA is a biocompatible polymer with thermal plasticity, semicrystalline with good mechanical, and seemingly good processing properties.[6–9] PLLA is widely used in many processing applications, including cast and blown film as well as thermoforming,[4,10] extrusion,[10,11] and injection molding.[5] However, PLLA melts has its debilities and generally do not exhibit the necessary strain hardening behavior, restricting its applications for processes that require high melt strength, such as extrusion coating, cast and blown film, as well as thermoforming.[4,5,10] Improved melt processability can be achieved through use of linear polymers in combination with branched polymers to enhance melt strength and stabilization.[6,12–15] Branching and modification for enhanced melt flow properties of polyethylene,[16,17] polypropylene,[18,19] polycaprolactone,[20] as well as polylactide[15] have been studied extensively. PLLA has also been modified by blending with a second polymer,[21,22] in order to improve processability or with a polymeric plasticizer such as polyethylene glycol (PEG). In high contents (more than 20%), PEG shows phase separation and it is not stable in the PLA matrix as a blend.[23] Wang *et al.* showed that the overall crystallization of linear PLLA will be higher comparing to the branched PLLA; moreover, the crystallization rate as well as melt temperature in both linear and sPLLA increased by increase in molecular weight.[14] Sakamoto *et al.*[24] studied linear 2-arm PLLA and branched 4-arm PLLA, and reported higher cold crystallization temperature (T_{cc}) values, lower degree of crystallinity (X_c), and lower spherulite growth rate for 4-arm compared to linear 2-arm PLLA. They showed that the glass transition temperature (T_g), melting temperature (T_m), transition crystallization temperatures of crystalline form, and crystal growth mechanism were not affected by the presence of branching; however, they are dependent on the M_n or M_n per one arm, which was in agreement with Wang *et al.* observations.[14] Some studies on blends with linear PLLA and star-shaped have been reported. However, the information on the blends rheological properties and the impact on the extrusion coating process are very limited.[25–32] Noteworthy, the requirements of the applications, e.g., food packaging, limit the choice of applicable polymers or plasticizers to modify the PLLA. Additives should not be volatile because this cause evaporation at the high processing

Table I. Characterizations of Synthesized sPLLAs

	DSC							SEC			^{1}H-NMR
Star-PLAs	T_c (°C)/X_c[a]	T_g (°C)[b]	T_{cc} (°C)[b]	T_m (°C)[b]	X_{cc}[b]	X_m[b]	T_i (°C)[b]	~M_n	~M_w	~PD	~M_n
S1	NA	34.4		Amorphous			215	2400	2700	1.14	2500
S2	NA	43.2	113	136	5	5	225	5400	8300	1.55	5500
S3	NA	53.1	110	147-156	39	39	228	11,500	19,000	1.65	12,000
S4	94.3/3	57.4	104	167	40	45	230	14,600	38,000	2.61	15,000
S5	95.4/25	57	97	168	25	49	240	33,400	55,000	1.65	35,000

[a] Determined from first cooling run.
[b] Determined from second heating run.
X_c (%) = $\Delta H_c/\Delta H_{m0} \times 100$.
X_{cc} (%) = $\Delta H_{cc}/\Delta H_{m0} \times 100$.
X_m (%) = $\Delta H_m/\Delta H_{m0} \times 100$.

temperatures. Furthermore, the additives should not be disposed to migration which would cause possible contamination and of course, possess food contact approval.[14]

In the current work, a series of star-shaped polylactide with different branch length have been prepared by ring-opening polymerization and blended with linear polylactide (PLLAs) produced by NatureWorks LLC, with the trade name 3051D.[4] The performance of these blends in extrusion coating is of particular interest. The main focus of this work is increase in the melt viscosity while the linear PLLA 3051D is plasticized. The thermal and rheological properties as well as phase behavior of linear PLLA blends containing 10 and 30 wt % of sPLLAs studied using differential scanning calorimetry and dynamic rheology. Overall use of star-shaped PLLA in the blend has modified the runability, heat sealability, and barrier properties due to increase in melt viscosity, at the same time, thermal stability improved by branching of polymer and shifting the start of degradation temperatures to higher temperatures, respectively.

EXPERIMENTAL

Materials

L-Lactide (Purac Biomaterials, Netherlands) was recrystallized from toluene before use. Pentaerythritol (PERYT) were used as a co-initiator and Sn(II) 2-ethylhexanoate as a catalyst (both from Sigma Aldrich, USA) without further treatment. Chromatography grade tetrahydrofuran (THF), $CDCl_3$, toluene, ethanol, and chloroform were purchased from Sigma-Aldrich USA; all chemicals were used as received. The polylactide was supplied as granular pellets by NatureWorks LLC, USA (commercial grade 3051D).

SYNTHESIS OF sPLLA AND PREPARATION OF BLENDS

The polymerization of star-PLLA was performed in a flame-dried and nitrogen-purged 250 mL flask reactor with magnetic stirring. First, L-lactide monomer was fed to the reactor with an appropriate amount of PERYT. The amount of co-initiators (PERYT) was calculated based on aimed molecular weight which varied between 2000 and 100,000 using eq. (1).[33]

$$\text{Amounts of Co-initiator} = (\text{L-lactide} \times \text{Efficiency} \times 74) / (\text{Total aimed Mw}) \quad (1)$$

After repeated evacuation and purge with nitrogen, the reactor was immersed into an oil bath at 160°C under nitrogen atmosphere.[33] The polymerization was initialized by injection of 0.05 mol % $Sn(Oct)_2$ from $Sn(Oct)_2$/toluene solution (10 wt %), reaction time were 60–75 min. The reaction was terminated by cooling the reactor to room temperature. The polymers were dissolved in chloroform and precipitated into a 10-fold excess of cold ethanol, isolated by filtration, and dried under vacuum (133 KPa) at 32.4°C overnight. All blends were prepared in solution using chloroform (24 h), then evaporated at 50°C, and further dried under vacuum (133 KPa) for 24 h. SPLLAs were mixed with linear PLLA (3051D) at mass ratios of 10 and 30 wt %. Prior to blending, sPLLAs and 3051D were dried in vacuum (133 KPa) overnight at 32.4°C.

Analytical Methods

^{1}H-NMR spectra were recorded on a Bruker AV 600 M in CDCl3 at 25°C and the peak positions are reported with respect to tetramethylsilane (TMS). Molecular weight and molecular weight distribution of all star-PLAs were obtained by size exclusion chromatography (SEC) using evaporative light scattering detector (ELS). Polymer solutions were prepared with 1 mg mL^{-1} of chloroform and filtered through a PTFE 0.2 μm filter. Fifty microliters of the samples were eluted at 40°C using auto injector system with a flow rate of 1 mL min^{-1}. Differential scanning calorimetric (DSC) measurements were performed on a calorimeter (TA instruments Q1000 Differential Scanning Calorimeter) in standard aluminum pans under an N_2 atmosphere. All samples were heated from −60 to 200°C and cooled down to −60°C at a rate of 10°C min^{-1} and then reheated to 200°C. The T_g (glass transition temperature), T_{cc} (temperature of cold crystallization), T_m (melting temperature), T_i (the initiation of degradation temperature for samples obtained by DSC in a separate run from −60 to 250°C), and ΔH_m (enthalpy of fusion) were taken from the second heating curve to eliminate the effect of thermal history. Three crystallinities were determined.

The crystallinity which appeared at cooling ramp (X_c) was calculated using X_c (%) = $\Delta H_c/\Delta H_{m0} \times 100$, the crystallinity at cold crystallization (X_{cc}) was calculated using X_{cc} (%) = $\Delta H_{cc}/\Delta H_{m0} \times 100$ and the crystallinity on melting (X_m) was calculated using X_c (%) = $\Delta H_m/\Delta H_{m0} \times 100$, where ΔH_m is the

enthalpy of fusion and ΔH_{m0} is the enthalpy of fusion of 100% crystalline PLA (93 J g^{-1}).[34] Rheological measurements were performed with a rotational rheometer (TA Instruments AR2000) using a parallel-plate geometry. Isothermal frequency sweeps were carried out at 240°C under nitrogen, using a 25 mm parallel-plate geometry and the gap was set to 1 mm. The applied strain and frequency range were 0.125% and 100–0.5 Hz, respectively. The steady-state flow step was also measured using the same parallel-plate geometry using shear rates ($\dot{\gamma}$) from 0.005 to 175 s^{-1}. The viscoelastic parameters, namely, storage modulus (G'), loss modulus (G''), complex viscosity (η^*), loss angle (δ), and shear viscosity (η) were calculated by using TA Data analysis software.

RESULTS AND DISCUSSION

Synthesis and Molecular Characterization of sPLLAs

The ring-opening polymerization of L-LA was carried out using pentaerythritol (PERYT) as a tetra-functional initiator and $Sn(Oct)_2$ as catalyst at 160°C for 60–75 min.[33]

Molecular characterization of sPLLA samples, determined by SEC and ^{1}H-NMR, are listed in Table I. Based on ^{1}H-NMR, it is obvious that star-shaped poly L-lactide (sPLLA) has been attained.[24,33] The results clearly indicate that the average number-molecular weight of the polymers obtained from SEC were in good agreement with the average number-molecular weight based on ^{1}H-NMR data. Though, in the case of the higher molecular weight samples, the obtained molecular number average was slightly lower than expected based on feeding ([M] $[I]^{-1}$).

Thermal and Rheological Properties of sPLLAs. DSC was used to examine the thermal properties and crystallization behavior of sPLLA and their blends with PLLA-3051D. The DSC curves of all sPLLA during the first cooling scan and the subsequent heating scan are shown in Figure 1.

Three sets of crystallinity data for the sPLLAs are presented in Table I: crystallinity formed during cooling X_c (%), crystallinity at cold-crystallization, X_{cc} (%) during the second heating, and total crystallinity at melting, X_m (%) which is a combination of the two other crystallization processes.

Concerning pristine sPLLAs, only small, hardly detectable exothermic crystallization peaks in the cooling ramp, X_c (%) were observed, except for two sPLLA samples, S4 and S5, revealing clear crystallization peaks centered at around 95°C [Figure 1(A)]. The second heating scan showed a glass transition, T_g, centered at 34°C for S1 and the T_g increased gradually with increasing molecular weight of the sPLLA to 57°C for S5. A broad exothermic (cold crystallization) peak centered at 113°C (T_{cc}) was displayed for S2 and the T_{cc} decreased gradually with increasing molecular weight to 97°C for S5. The S1 remained amorphous, while a broad endothermic (melting) peak centered at 136°C was displayed for S2 ($\Delta H_m = 5$ J g^{-1}) increasing to 40 J g^{-1} for S4. However, S5 showed a lower cold crystallization ($\Delta H_{cc} = 25$ J g^{-1}) mostly due to its higher degree of crystallization at cooling, X_c, of 25 J g^{-1}. This shows that 4-arm PLLA with longer branch lengths crystallize more easily during the cooling and heating process. A significant increase in the melting temperature (T_m) of 30°C was detected with increasing molecular weights from S2 to S5. Notably, sPLLA with higher molecular weights, S3 and S4, exhibit two visible melting endotherms [Figure 1(B)]. It is believed that multiple melting peaks are often related to crystals with different degrees of perfection. As shown in Figure 1(B), the intensity of the T_{m2} peak (156°C) was higher than that of the T_{m1} peak (147°C) for samples S3 and S4; however, S5 exhibited only one melting peak (168°C). Thus, the intensity ratio of T_{m2} to T_{m1} peaks increased with branch length. Initial degradation temperature T_i shown in the second heating scan in Figure 1(B) started at 215°C for S1 and the T_i increased gradually with increasing molecular weight of the sPLLA to 240°C for S5. Notably, 3051D showed T_i at 210°C which is lower than all sPLLAs.

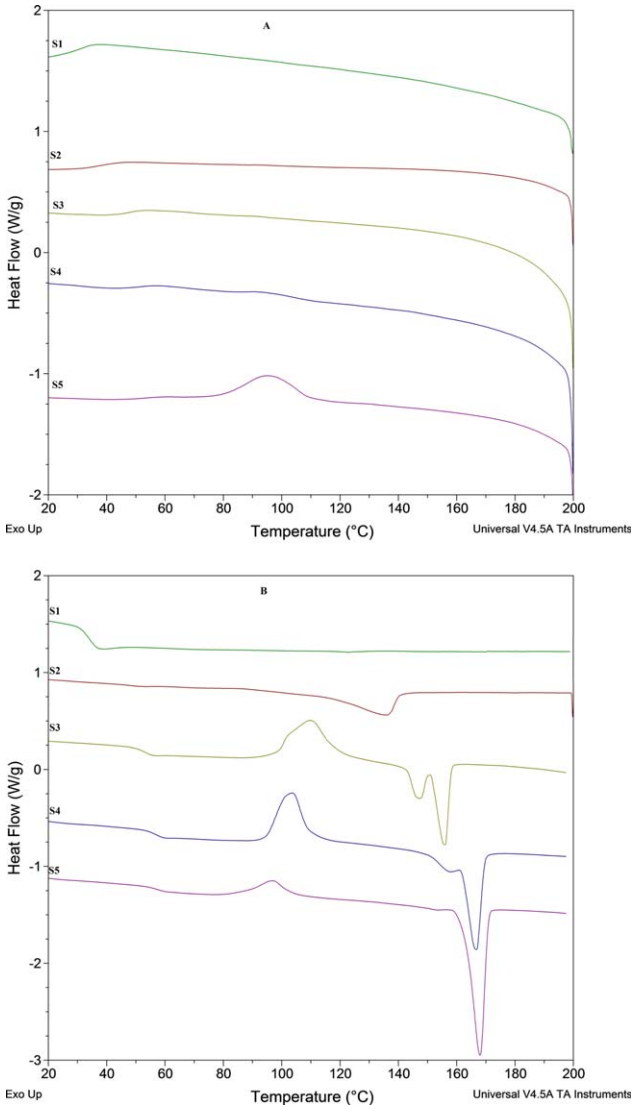

Figure 1. DSC curves of sPLLAs: (A) the first cooling scan and (B) the second heating scan. [Color figure can be viewed in the online issue, which is available at wileyonlinelibrary.com.]

From these results, it can be concluded that the structure and molecular weight of the sPLLA polymers plays a significant role

in the process of crystallization. sPLLAs can be appropriate and helpful for faster crystallization during cooling because the branch points can act as nucleating centres to accelerate crystallization. Nevertheless the perfection of the crystals might be disturbed as a result because branched PLAs are less capable of increasing the lamellar thickness due to their restricted mobility in comparison with linear PLLA.[35] Four-arm PLLA were synthesized according to Korhonen *et al.*,[22] though with different molecular weights comparing to their research and compared with Wang *et al.*[14] and Sakamoto *et al.*[24] The T_g (indicator of chain mobility), T_{cc} (indicator of ability to crystallize during heating), T_m (indicator of crystalline thickness), T_i (indicating initial thermal degradation), and ΔH_m (indicator of final degree of crystallinity during heating) of the sPLLAs increased with increasing M_w except for S1 with the lowest molecular weight, in which neither a cold crystallization nor a melting peak was observed, in Figure 1. The rheology of pure star-shaped PLLA was analyzed at 190°C using a Bohlin Vor Rheometer (rotational rheometer). The shear viscosity of low M_w star-shaped polymers is lower than for its corresponding linear polymer with similar molecular weight due to higher segment density and reduced hydrodynamic volume.[15] However, the viscosity of the star-shaped polymer increases faster with the molecular weight and surpasses that of the linear analog at some specific molecular weight, as the star-shaped polymer possesses restricted chain mobility due to chain entanglements and motional constraints as one end of the arm is anchored to the star core.[15]

The rheological properties of the low molecular weight samples S1 and S2 were not measureable at 190°C because of their very low shear viscosity; therefore, they had to be analyzed at 150°C. The viscosity curves of the neat star-shaped polymers (not included) showed an obvious influence of the molecular weight on the flow properties. A higher M_w yielded a slightly higher zero shear viscosity (η_0), also with a more pronounced shear thinning behavior.

In a shear field, the larger object dissipates more energy, resulting in a higher viscosity. Consequently, star-shaped polymer's larger hydrodynamic volume compare to comparable linear one would naturally lead to a higher viscosity.[36] Nonetheless, all our star-shaped polymers have lower shear viscosities compared to linear 3051D ($M_w = 121{,}000$ and MWD = 2.59), due to their substantially lower molecular weights (M_w 2500–35,000 g mol^{-1}) and denser structures.

Blends of sPLLA and Linear PLLA

A series of sPLLAs with increasing arm lengths (molecular weights) were synthesized and their blends were prepared via solution blending with the content of 70 and 90 wt % of commercial 3051D PLLA (NatureWorks LLC). The basic information on the neat polymers is listed in Table I. Three sPLLA—low, medium, and high molecular weight (2500, 12,500, and 35,000 g mol^{-1})—have been chosen for further rheological analysis as blends with the linear PLLA at 240°C.

As well known, entanglements between molecular chains in molten polymers can be enhanced by introducing branched structures to the polymer resin, thereby distinctly enhancing the melt strength/elasticity. Improving melt processability of polymer resin by increasing melt strength and melt elasticity is well understood and has been evaluated for different materials.[37,38] Effects of randomly branched PLLA by reactive extrusion with different peroxides have been studied in our previous work.[39] Peroxide treatment is often connected with cross-linking/gelation of the polymer which may severely endanger melt processing, e.g., in extrusion coating. Therefore, it would be important and desirable to control the quality and degree of branching in the polymer.

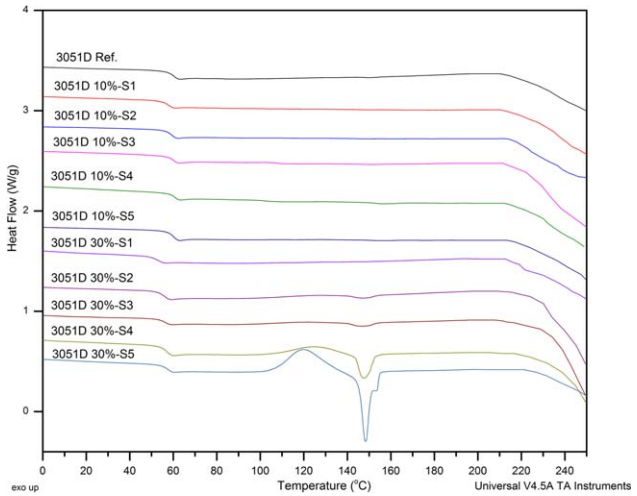

Figure 2. DSC curves of star-PLA blends from the second heating scan. [Color figure can be viewed in the online issue, which is available at wileyonlinelibrary.com.]

To obtain more identical conditions with materials going through a dry-blending process during an extrusion coating, the sPLLA have been mixed in solution with 3051D PLLA, so that they are melted (dry-blended) for the first time in the rheometer under the same conditions as in the anticipated extruder dry-blending with 3051D pellets.

Thermal and Rheological Properties of sPLLA Blends

Thermal Properties. The thermal characterization of sPLLA blends were determined by DSC. The glass transition temperatures of neat star-shaped polymers S1–S5 were 34.4, 43.2, 53.1, 57.4, and 57°C, respectively, while the T_g of pure 3051D is 60°C (Tables I and II). Qiu *et al.* studied the crystallization and miscibility of different biopolymer blends.[40] They studied the miscibility by the composition dependency on T_g, change of T_m, and cold crystallization temperature. The T_g values of the present PLLA blends with S1–S3 are slightly dependent on the blend composition, proving that the binary blends are partially miscible.[40,41] This suggests that sPLLA acts as a plasticizer in linear PLLA. Especially, a significant depression of T_g by 7°C (12% reduction) was observed in PLLA with 30 wt % of S1, which is a typical behavior for plasticized semicrystalline polymers. The glass transitions of the blends reveal the interactions between the respective polymers in blends. Particularly, some level of compatibility may be interpreted when the two separately observed T_gs are shifted toward each other or just one T_g appears in a binary polymer blend.[42] It has to be mentioned

Table II. Thermal Properties of 3051D/ Star-PLA Blends

	DSC				
Samples	T_g (°C)	T_m (°C)	T_c (°C)/X_{cc}	X_m	T_i (°C)
3051D/10%-S1	57		Amorphous		210
3051D/10%-S2	59		Amorphous		211
3051D/10%-S3	60		Amorphous		212
3051D/10%-S4	61		Amorphous		212
3051D/10%-S5	60		Amorphous		214
3051D/30%-S1	53		Amorphous		213
3051D/30%-S2	56	147	123/1.6	1.6	215
3051D/30%-S3	57	147	121/5	5	216
3051D/30%-S4	60	148	124/10	10	219
3051D/30%-S5	60	148-152	120/30	30	222
3051D Ref.	60		Amorphous		210

All data are determined from second heating run.
X_{cc} (%) = $\Delta H_{cc}/\Delta H_{m0} \times 100$.
X_m (%) = $\Delta H_m/\Delta H_{m0} \times 100$.

that T_g of PLLA 3051D, S4, and S5 are so close, 60, 57.4, and 57°C, respectively, that it is ambiguous to conclude if any depression of T_g have appeared in the blends. The first heating scan of pristine linear PLLA pellets showed an endothermic peak (melting, $T = 149$°C, not shown), but no detectable melting in the second heating scan. The curves of the second heating scan of all blends containing 10% of sPLLAs and 30% of S1 samples displayed one glass transition temperature (T_g) centered at 53–61°C implying compatibility of these blends. Though, no crystallization was detected during the cooling ramp followed by an amorphous plateau showing that sPLLAs in the used concentrations could not crystallize neither improve the crystallization of pure PLLA (Figure 2). Initial degradation temperature (T_i) of the PLLA 3051D and corresponding blends with sPLLA are shown in Figure 2 and Table II. PLLA 3051D showed a T_i at 210°C and addition of 10 wt % S1–S5 increased the T_i slightly from 210 to 214°C, respectively. Remarkably, blends with 30 wt % of sPLLAs displayed increment from 215°C for S1 to 222°C for 30% S5. Initial degradation temperature is a sign of thermal stability of polymers. Notably, 3051D showed a T_i at 210°C which is lower than all sPLLAs and their blends emphasizing an improvement of thermal stability by using star-shaped structure.

As shown in Figure 2 and Table II, an addition of 30 wt % of S2–S5 exhibited exothermic peaks at 120–125°C (cold crystallization, T_{cc}), and a broad endothermic peak at 147–152°C (melting, T_m) also only one T_g is observed suggesting compatibility in the blend. No significant influence on the crystallization of the PLLA 3051D was observed since the amounts of total crystallinity equalizes to the proportion of crystalline sPLLAs in the blend. However, the crystallization on heating (annealing) of the blend of S5–30 wt % was 30%, which is nearly doubled as estimated based on the content of S5 and a sharp melting peak appeared which would be sign of melting of linear PLLA (Figure 2). Therefore, one could conclude that S5 increased ability of 3051D to crystallize on the heating ramp. This would be due to the reorganization of amorphous segments into crystalline ones, as a result of increased macromolecular freedom upon increasing temperature.[43]

The heat of melting (ΔH_m) and the exothermal heat of crystallization (ΔH_c) of the blends were found to increase with an increased concentration and size of the sPLLA. The temperature of the melting peak shifted toward higher temperature as the M_w of the sPLLA increased. A double endotherm was observed for 3051D with S5–30 wt %, implying the existence of two different crystals in this blend, likely due to perfection issues resulting from disturbed crystallization or melting of the linear PLLA. Therefore, authors believe that 30 wt % of S5 could significantly affect crystallinity of 3051D as compared with blends containing lower concentrations and lower molecular weight sPLLA. Comparing the thermal behavior of the pure PLLA and sPLLA with the corresponding blends, the T_g value was attributed to the combined sPLLA/3051D amorphous domains. The exothermic peaks owe to the crystallization of sPLLA blocks, and the broad endothermic peak due to the overlapping of the melting temperature of the crystallites with different crystalline size.[24]

Rheological Properties. To understand the melt flow properties of the PLLA blends, a detailed investigation of the rheological behavior of these blends with varying sPLLA concentration was done, performing the rheological measurements at 240°C to mimic the extrusion conditions at industrial processes. The analyses were performed under nitrogen atmosphere in order to minimize thermal oxidation. All blends were mixed in solution (chloroform) and dried, in order to avoid premature thermal degradation and to obtain the "true" material behavior during its first melting (as it would be in the case of a dry mix during extrusion). Thus, the results are comparable with the material properties at an extrusion coating processes. The main focus has been on the rheological properties such as storage modulus (G'), loss modulus (G''), complex viscosity (η^*), and shear viscosity (η). The storage modulus G' reflects the elastic part and

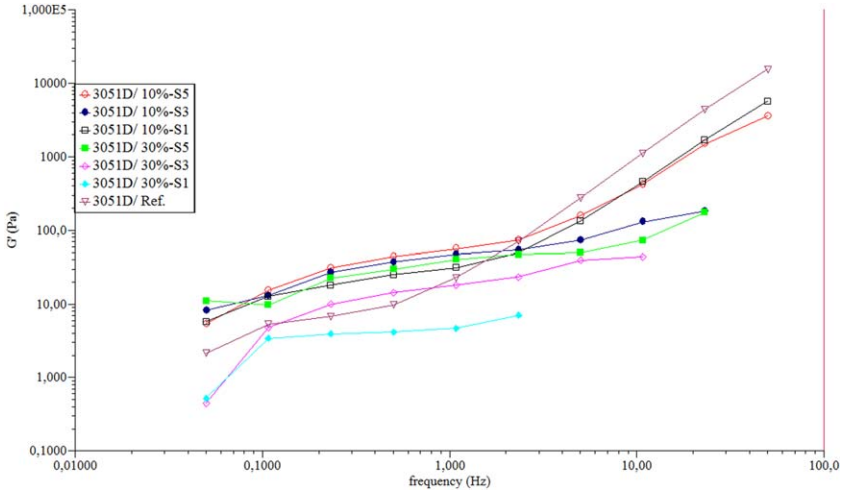

Figure 3. Storage modulus as a function of frequency for linear PLA 3051D and star-PLA blends with different molecular weight and concentrations. [Color figure can be viewed in the online issue, which is available at wileyonlinelibrary.com.]

loss modulus G'' the viscous part of polymer melts. Branching is often introduced to polymeric material to modify the flow properties for specific melt-forming operations. It is well understood that when the branch length exceeds some critical value, it leads to an increase in the viscosity compared to the linear molecule with the same molecular weight due to entanglements by the branches.[44]

Complex viscosity and storage modulus of PLLA 3051D and blends are shown in Figure 3. It is clear that PLLA 3051D exhibit terminal flow behavior at low frequency in the dynamic storage modulus (G') and loss modulus (G''), i.e., scales to $G' \alpha \omega^2$ and $G'' \alpha \omega$, respectively, which are characteristics for a viscoelastic liquid. For all blends containing 10 wt % of sPLLAs and 30% of S5, a shoulder (deflection in curve slope) on the G' curve is seen (frequency ~2 Hz) which indicates that the storage modulus exhibit weak frequency dependency at moderately low frequencies. This nonterminal behavior indicates the presence of a longer relaxation process not detected in the linear PLLA. It should correspond to the "additional" elastic response originating from the surface interaction between the droplets (sPLLA) in the discrete phase and the continuous matrix (linear PLLA), and has been reported for many blends with lower level of miscibility or immiscible blends.[45] Similar results were reported by Lee *et al.*[46] with experimental values of the G' obtained from either phase separated or degraded polymer blends. This result could be examined together with complex viscosity frequency dependence of the same blends (Figure 4). The complex viscosity increases as the frequency decrease, as is typical for yield stress fluids, i.e., from 20 Pas to 70 Pas. The slopes of log G' vs log ω for the pure PLLA and blends with 30% of S1 and S3 were close to 2, respectively, which is similar to the behavior of thermorheologically simple polymers in the terminal regime implying miscibility in these blends (Figure 3).[47] This shows that the blend ratio and the interface between PLA and sPLLA play an important role in the

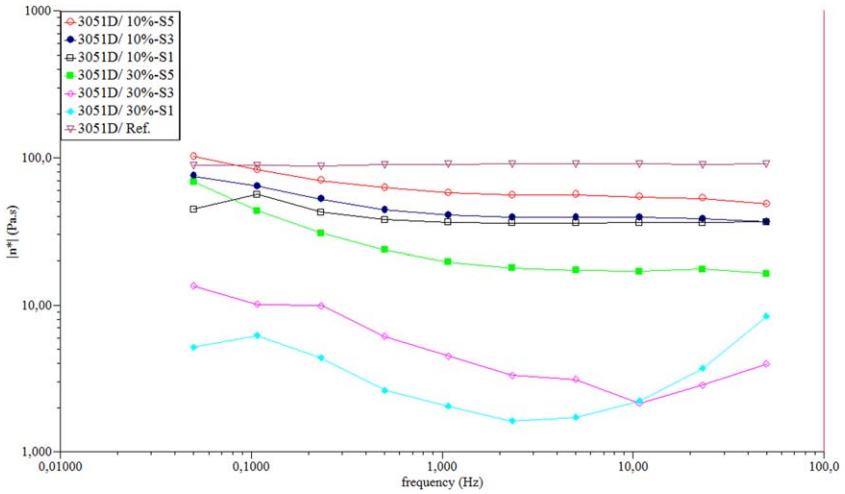

Figure 4. Complex viscosity as a function of frequency for linear PLA 3051D and star-PLA blends with different molecular weight and concentrations. [Color figure can be viewed in the online issue, which is available at wileyonlinelibrary.com.]

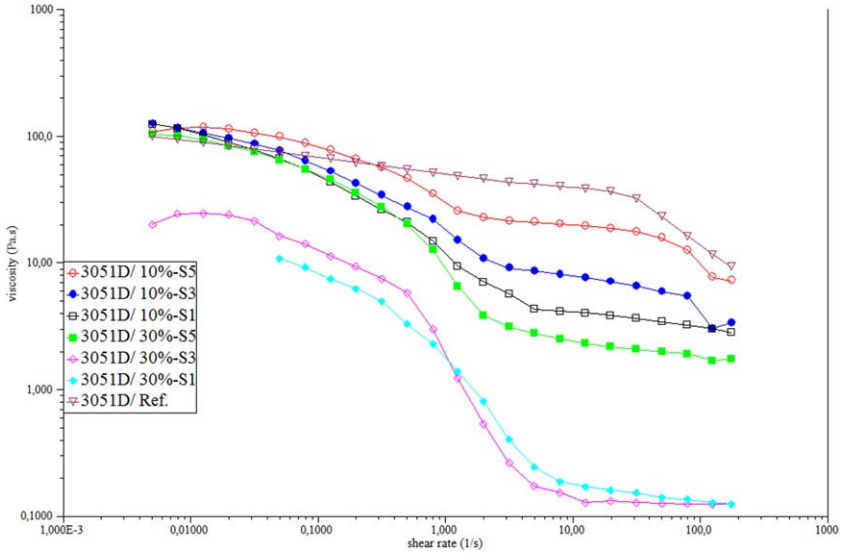

Figure 5. Shear viscosity as function of shear rates for linear PLA 3051D and star-PLA blends with different molecular weight and concentrations. [Color figure can be viewed in the online issue, which is available at wileyonlinelibrary.com.]

viscoelastic response of these blends. However, more study is needed to better understanding of the specific viscoelastic response of the blends observed at lower frequencies.

The shear viscosity of a molten polymer typically displays a constant value at very low shear rates (zero shear viscosity η_0), and which begins to deviate from η_0 at some characteristic shear rate (non-Newtonian). Figure 5 summarizes the shear viscosity (η) of linear PLLA and its blends with sPLLAs at 240°C. Linear PLLA has a zero shear viscosity η_0 of about 100 Pas and approaches power law behavior at higher shear rates. Blends containing 10% of all sPLLAs and 30% of S5 show zero shear viscosity (η_0) similar to linear PLLA (3051D) as well as shear thinning starting almost immediately (shear rate of ~0.1 s^1), and finally leveling to different, rather constant viscosities, 2 Pas at 30% of S1 to 30 Pas for 10% of S5. This points out that total molecular weight of these blends remained rather unaffected, while their polydispersity has increased. In case of blends with 30% of S1 and S3, the zero shear viscosity decreased one order of magnitude (from 100 to 20 Pas) which indicates declined total molecular weight. These blends also showed shear thinning beginning at shear rates of ~0.1 s^1, and finally the viscosity decreased to a very low viscosity of about 0.1 Pas. These latter blends showed a larger range of viscosity values due to stronger shear thinning which is attributed to plasticizing effects of low-molecular-weight sPLLAs at this concentration.

The rheological properties showed that beside linear PLLA, the blends can be divided into two categories: blends containing 10% sPLLA and PLLA with 30% of S5 showed some level of immiscibility and blends with 30% of S1 and S3 which appears more homogeneous and miscible.

CONCLUSION

Star-shaped (4-arm) PLLAs, with various total molecular weights were synthesized using pentaerythritol. The sPLLAs structures were confirmed by ^{1}H-NMR spectroscopy and characterized with dynamic rheology, DSC, and size-exclusion chromatography. The sPLLAs were further blended with commercial PLLA by solvent mixing. Miscibility, morphology, and rheological behavior of the blends were investigated by DSC, steady shear flow, and dynamic rheology. Star-shaped PLLA showed higher thermal stability and the initial degradation temperature of linear PLLA was increased by blending with sPLLA, which proves that blending improved the thermal stability of linear PLLA 3051D. All blends appear to have some level of compatibility since only one T_g have been observed. However, based on the thermal and rheological characteristics of the studied blends, two different morphologies were observed: first blends containing 10% of all sPLLAs or 30% of S5, which showed slightly immiscibility and partially a two-phased morphology, and second, miscible and homogenous blends containing 30% of S1 and S3. The interface between two polymers plays an important role in the viscoelastic response of molten sPLLA/ linear PLLA blends. It could be concluded that miscibility, phase behavior, and crystallization of the blends were influenced significantly by amounts and type of the added sPLLAs, as we postulate sPLLA can act as a nucleating agent due to its branched structure. Blending of 3051D with 5 and 10% of S5 was tested on an extrusion coating pilot line. Star-shaped polymer seems to enhance heat sealability but not neck-in or adhesion. Water vapor transmission rate (WVTR) was similar to pure 3051D but in the lower concentration, WVTR was increased.

ACKNOWLEDGMENTS

The authors wish to thank the Finnish Funding Agency for Technology and Innovation (TEKES) for financial support and Jurkka Kuusipalo and Sami Kotkamo from Tampere University of Technology for testing with the pilot line. We also wish to extend our sincere appreciation to Stora Enso.

REFERENCES

1. Perepelkin, K. E. *Fibre Chem.* **2002**, *34*, 85.
2. Datta, R.; Henry, M. *J. Chem. Technol. Biotechnol.* **2006**, *81*, 1119.
3. Davachi, S. M.; Kaffashi, B. *Polym. Plast. Technol. Eng.* **2015**, to appear..
4. Cock, F.; Cuadri, A. A.; García-Morales, M.; Partal, P. *Polym. Test.* **2013**, *32*, 716.
5. Lim, L.-T.; Auras, R.; Rubino, M. *Prog. Polym. Sci.* **2008**, *33*, 820.
6. You, J.; Lou, L.; Yu, W.; Zhou, C. *J. Appl. Polym. Sci.* **2013**, *129*, 1959.
7. Davachi, S. M.; Kaffashi, B. *Int. J. Polym. Mater.* **2015**, *64*, 497.
8. Davachi, S. M.; Kaffashi, B.; Roushandeh, J. M.; Torabinejad, B. *Mater. Sci. Eng. C* **2012**, *32*, 98.
9. Davachi, S. M.; Kaffashi, B.; Roushandeh, J. M. *Polym. Adv. Technol.* **2012**, *23*, 565.
10. Shiromoto, S.; Masutani, Y.; Tsutsubuchi, M.; Togawa, Y.; Kajiwara, T. *Rheol. Acta* **2010**, *49*, 757.
11. Hartmann, M.; Whiteman, N. In Technical Papers of The Annual Technical Conference-Society of Plastics Engineers Incorporated; **2001**; Vol. 1, p 2.
12. Liu, J.; Lou, L.; Yu, W.; Liao, R.; Li, R.; Zhou, C. *Polymer* **2010**, *51*, 5186.
13. Wang, Y.; Yang, L.; Niu, Y.; Wang, Z.; Zhang, J.; Yu, F.; Zhang, H. *J. Appl. Polym. Sci.* **2011**, *122*, 1857.
14. Wang, L.; Jing, X.; Cheng, H.; Hu, X.; Yang, L.; Huang, Y. *Ind. Eng. Chem. Res.* **2012**, *51*, 10731.
15. McKee, M. G.; Unal, S.; Wilkes, G. L.; Long, T. E. *Prog. Polym. Sci.* **2005**, *30*, 507.
16. Groves, D. J.; McLeish, T. C.; Chohan, R. K.; Coates, P. D. *Rheol. Acta* **1996**, *35*, 481.
17. Kim, J.; Kim, D. H.; Son, Y. *Polymer* **2009**, *50*, 4998.
18. Tabatabaei, S. H.; Carreau, P. J.; Ajji, A. *Chem. Eng. Sci.* **2009**, *64*, 4719.
19. McCallum, T. J.; Kontopoulou, M.; Park, C. B.; Muliawan, E. B.; Hatzikiriakos, S. G. *Polym. Eng. Sci.* **2007**, *47*, 1133.
20. Wang, L.; Ma, W.; Gross, R. A.; McCarthy, S. P. *Polym. Degrad. Stab.* **1998**, *59*, 161.
21. Bhatia, A.; Gupta, R.; Bhattacharya, S.; Choi, H. *Korea-Aust. Rheol. J.* **2007**, *19*, 125.
22. Gu, S.-Y.; Zhang, K.; Ren, J.; Zhan, H. *Carbohydr. Polym.* **2008**, *74*, 79.
23. Baiardo, M.; Frisoni, G.; Scandola, M.; Rimelen, M.; Lips, D.; Ruffieux, K.; Wintermantel, E. *J. Appl. Polym. Sci.* **2003**, *90*, 1731.
24. Sakamoto, Y.; Tsuji, H. *Polymer* **2013**, *54*, 2422.
25. Odelius, K.; Albertsson, A.-C. *J. Polym. Sci. Part A: Polym. Chem.* **2008**, *46*, 1249.
26. Karikari, A. S.; Edwards, W. F.; Mecham, J. B.; Long, T. E. *Biomacromolecules* **2005**, *6*, 2866.
27. Salaam, L. E.; Dean, D.; Bray, T. L. *Polymer* **2006**, *47*, 310.
28. Adeli, M.; Zarnegar, Z.; Kabiri, R. *Eur. Polym. J.* **2008**, *44*, 1921.
29. Lin, W.-J.; Chen, Y.-C.; Lin, C.-C.; Chen, C.-F.; Chen, J.-W. *J. Biomed. Mater. Res. B Appl. Biomater.* **2006**, *77*, 188.
30. Pitet, L. M.; Hait, S. B.; Lanyk, T. J.; Knauss, D. M. *Macromolecules* **2007**, *40*, 2327.
31. Cai, Q.; Zhao, Y.; Bei, J.; Xi, F.; Wang, S. *Biomacromolecules* **2003**, *4*, 828.
32. Dorgan, J. R.; Janzen, J.; Knauss, D. M.; Hait, S. B.; Limoges, B. R.; Hutchinson, M. H. *J. Polym. Sci. Part B Polym. Phys.* **2005**, *43*, 3100.
33. Korhonen, H.; Helminen, A.; Seppälä, J. V. *Polymer* **2001**, *42*, 7541.
34. Mohammadi-Rovshandeh, J.; Pouresmaeel-Selakjani, P.; Davachi, S. M.; Kaffashi, B.; Hassani, A.; Bahmeyi, A. *J. Appl. Polym. Sci.* **2014**, 131.
35. He, Y.; Fan, Z.; Hu, Y.; Wu, T.; Wei, J.; Li, S. *Eur. Polym. J.* **2007**, *43*, 4431.
36. Nunez, C. M.; Chiou, B.-S.; Andrady, A. L.; Khan, S. A. *Macromolecules* **2000**, *33*, 1720.
37. Dean, K. M.; Petinakis, E.; Meure, S.; Yu, L.; Chryss, A. *J. Polym. Environ.* **2012**, *20*, 741.
38. Ryan, C. M.; Hartmann, M. H.; Nangeroni, J. F. In Polymers Laminations and Coatings Conference; Tappi Press: Toronto, Ontario; **1997**; p 139.
39. Khajeheian, M. B.; Rosling, A. *J. Polym. Environ.* **2015**, *23*, 62.
40. Qiu, Z.; Fujinami, S.; Komura, M.; Nakajima, K.; Ikehara, T.; Nishi, T. Macromolecular Symposia. Contributions from 8th Pacific Polymer Conference; **2004**; Vol. 216, p 255.
41. Zuideveld, M.; Gottschalk, C.; Kropfinger, H.; Thomann, R.; Rusu, M.; Frey, H. *Polymer* **2006**, *47*, 3740.
42. Martin, O.; Averous, L. *Polymer* **2001**, *42*, 6209.
43. Signori, F.; Coltelli, M.-B.; Bronco, S. *Polym. Degrad. Stab.* **2009**, *94*, 74.
44. Blottiere, B.; McLeish, T. C. B.; Hakiki, A.; Young, R. N.; Milner, S. T. *Macromolecules* **1998**, *31*, 9295.
45. Graebling, D.; Muller, R.; Palierne, J. F. *Macromolecules* **1993**, *26*, 320.
46. Lee, J. H.; Ruegg, M. L.; Balsara, N. P.; Zhu, Y.; Gido, S. P.; Krishnamoorti, R.; Kim, M.-H. *Macromolecules* **2003**, *36*, 6537.
47. Sungsanit, K.; Kao, N.; Bhattacharya, S. N.; Pivsaart, S. *Korea-Aust. Rheol. J.* **2010**, *22*, 187.